Available online at www.sciencedirect.com
ScienceDirect
Ceramics International 37 (2011) 741–748
CERAMICS INTERNATIONAL
www.elsevier.com/locate/ceramint

Synthesis and characterization of clinopyroxene based glasses and glass-ceramics along diopside ($CaMgSi_2O_6$)–jadeite ($NaAlSi_2O_6$) join

Rinkel Jindal [a,b,*], R. Jayaganthan [a], Indra Vir Singh [c], Reinhard Conradt [b]

[a] Department of Metallurgical and Materials Engineering & Centre of Nano-technology, Indian Institute of Technology Roorkee, Roorkee 247667, India
[b] Department of Glass and Ceramic Composites, Institute of Mineral Engineering, RWTH Aachen, Mauerstr. 5, 52064 Aachen, Germany
[c] Department of Mechanical and Industrial Engineering, Indian Institute of Technology Roorkee, Roorkee 247667, India

Received 26 April 2010; received in revised form 6 May 2010; accepted 28 September 2010
Available online 11 November 2010

Abstract

The crystallization behavior and mechanical characterization of glasses based upon the compositions along diopside ($CaMgSi_2O_6$)–jadeite ($NaAlSi_2O_6$) join has been investigated. Six glasses were obtained by the melt-quenching technique. Structural and thermal behaviors of these glasses were investigated by density and molar volume, infrared spectroscopy (FTIR) and dilatometry. The crystallization behavior of glasses was investigated by using differential scanning calorimetry (DSC). Sintering and crystallization behavior of the glass-ceramics were investigated under non-isothermal heating conditions up to temperatures of 850 °C. Mechanical characterization of glasses was investigated by using the measurement of Vickers indentation hardness and elastic constants such as Young's modulus (E), shear modulus (G), bulk modulus (K) and Poisson's ratio (ν). These data of the glasses were correlated with the structure of glasses, nature and role played by glass forming cations.

Keywords: C. Mechanical properties; C. Hardness; D. Glass

1. Introduction

Pyroxenes are major constituents of earth's crust and of the upper mantle to depths of 400 km. The general chemical formula for pyroxenes is $M2M1T_2O_6$, where M2 refers to cations in a generally distorted octahedral coordination (Mg^{2+}, Fe^{2+}, Mn^{2+}, Li^{+}, Ca^{2+}, Na^{+}), M1 to cations in a regular octahedral coordination (Al^{3+}, Fe^{3+}, Ti^{4+}, Cr^{3+}, V^{3+}, Ti^{3+}, Zr^{4+}, Sc^{3+}, Zn^{2+}, Mg^{2+}, Fe^{2+}, Mn^{2+}), and T to tetrahedrally coordinated cations (Si^{4+}, Al^{3+}, Fe^{3+}). Any pyroxene belongs to either the orthorhombic or the monoclinic crystal system. Monoclinic pyroxenes are called clinopyroxenes. The chain structure of clinopyroxenes enables incorporation of various cations in their structure resulting in minerals founds in abundance in the nature, such as diopside ($CaMgSi_2O_6$), hedenbergite ($CaFeSi_2O_6$), aegirine ($NaFeSi_2O_6$), jadeite ($NaAlSi_2O_6$), spodumene ($LiAlSi_2O_6$), etc. [1].

The solid solution between diopside ($CaMgSi_2O_6$; hereafter referred as Di) and jadeite ($NaAlSi_2O_6$; hereafter referred as Jd) is a subject of relevance from petrologic as well as technological point of view. It is noteworthy that although Jd is metastable at one bar pressure and only forms at high pressure ($\geq$3 GPa), a stable solid solution exists between Di and Jd forming a C2/c monoclinic lattice and is one of the most important pseudo-binary chemical systems in petrology [2]. It is due to this reason that Di–Jd join has been an area under discussion among researchers for a considerable period of time. The binary phase diagram of Di–Jd system has been studied by Schairer and Yoder [3] at a pressure of 1 atm while many studies investigating the phase relations at high temperature and pressures in Di–Jd system have been reported [4–8]. Wood et al. [9] studied the thermo-chemistry of synthetic Di–Jd pyroxenes and found that the investigated synthetic clinopyroxenes have positive excess enthalpies of mixing. Also, it was reported that Di–Jd solid solutions are 'pseudo-ideal' near 1:1 composition at temperatures of 1000–1500 K. Recently, Abo-Mosallam et al. [2] studied the structure and crystallization behavior of glasses

* Corresponding author at: Department of Metallurgical and Materials Engineering & Centre of Nano-technology, Indian Institute of Technology Roorkee, Roorkee 247667, India. Tel.: +91 9820728228; fax: +91 22 2572 6975.
E-mail address: rinkeljindal@gmail.com (R. Jindal).

0272-8842/$36.00
doi:10.1016/j.ceramint.2010.09.049

Table 1
Batch composition of glasses.

Glass		MgO	CaO	Na_2O	SiO_2	B_2O_3	Al_2O_3
Jd-0	wt.%	18.97	26.40	–	48.08	6.55	–
$CaMgSi_{1.7}B_{0.4}O_6$	mol.%	25.65	25.65	–	43.57	5.13	–
Jd-20	wt.%	15.39	21.41	2.96	48.74	6.65	4.87
$Ca_{0.8}Mg_{0.8}Na_{0.2}Si_{1.7}Al_{0.2}B_{0.4}O_6$	mol.%	21.60	21.60	2.72	45.93	5.43	2.72
Jd-40	wt.%	11.7	16.28	6.0	49.42	6.74	9.87
$Ca_{0.6}Mg_{0.6}Na_{0.4}Si_{1.7}Al_{0.4}B_{0.4}O_6$	mol.%	17.12	17.12	5.73	48.57	5.73	5.73
Jd-60	wt.%	7.91	11.01	9.12	50.12	6.83	15.01
$Ca_{0.4}Mg_{0.4}Na_{0.6}Si_{1.7}Al_{0.6}B_{0.4}O_6$	mol.%	12.11	12.11	9.09	51.44	6.06	9.09
Jd-80	wt.%	4.01	5.58	12.34	50.84	6.93	20.3
$Ca_{0.2}Mg_{0.2}Na_{0.8}Si_{1.7}Al_{0.8}B_{0.4}O_6$	mol.%	6.42	6.42	12.92	54.90	6.42	12.92
Jd-100	wt.%	–	–	15.65	51.58	7.03	25.74
$NaAlSi_{1.7}B_{0.4}O_6$	mol.%	–	–	17.27	58.57	6.89	17.27

and glass-ceramics along $(CaMgSi_2O_6)_{1-x}$–$(NaAlSi_2O_6)_x$–$(Ca_5(PO_4)_3F)_y$ where $0 \leq x \leq 30$ mol.% and $y = 7$ mol.%. He has reported that with increase in Jd content in the glasses, the polymerization in silicate glass network shifted from Q^2 to Q^3 (Q^n: degree of polymerization; n: number of bridging oxygens) and Al exists predominantly as Al (IV) species. A complete solid solution has been reported to exist between Di–Jd glass-ceramics at 1 atm pressure for the first time in literature [2]. However, to the best of our knowledge, the structure and crystallization behavior in complete series of glasses along Di–Jd join have not been reported so far in open literature. Therefore, the primary aim of this study is to investigate the structural and mechanical properties of glasses along Di_{1-x}–Jd_x (x = 0–100 mol.%) join in conjunction with their sintering and crystallization behavior. It should be noted that small amounts of B_2O_3 have been added in all the investigated glasses in accordance with substitution Scheme $0.3Si^{4+} \leftrightarrow 0.4B^{3+}$, so as to decrease the viscosity of the glass melts and tailor the flow properties of the resultant glass-ceramics which can be useful for some technological applications related with coatings on ceramic/metallic substrates [10,11]. Table 1 presents the compositions of all the investigated glasses.

2. Experimental

Homogeneous mixtures of batches (∼200 g) in accordance with glass compositions presented in Table 1 were prepared by ball milling of powders of SiO_2 (Sigma–Aldrich, purity >99.7%), $CaCO_3$ (Merck, >99.8%), Al_2O_3 (Merck, ≥98%), H_3BO_3 (Merck, 99.8%), MgO (Merck, >99.7%), Na_2CO_3 (Merck, 99.9%), and calcination at 900 °C for 1 h. The glass batch was melted in Pt crucibles at 1500 °C for 1 h, in air. Glasses in bulk form were produced by pouring the melts on preheated graphite moulds followed by annealing at 550 °C for 1 h while glass frits were obtained by quenching of glass melts in cold water. The frits were dried and then milled in a high-speed agate mill resulting in fine glass powders with mean particle sizes of 10–20 μm (determined by light scattering technique; Coulter LS 230, Beckman Coulter, Fullerton CA; Fraunhofer optical model). The experimental glass compositions as determined by X-ray fluorescence (XRF, PW 2404 X-ray Spectrometer, Phillips, Netherlands) are presented in Table 2.

Archimedes' method (by immersion in ethylene glycol) was employed to measure the apparent densities of the bulk annealed glasses which was further employed along with compositions of glasses to calculate the molar volumes and excess volumes of glasses.

Infrared spectra for the glass powders were obtained using an Infrared Fourier spectrometer (FT-IR, model Mattson Galaxy S-7000, USA). For this purpose each glass powder was mixed with KBr in the proportion of 1/150 (by weight) and pressed into a pellet using a manual press.

The elastic constants (Young's modulus (E), shear modulus (G), bulk modulus (K) and Poison's ratio (ν) of glasses were determined by ultrasonic echography. For this purpose, velocities of longitudinal (10 MHz) and transverse (4 MHz) ultrasonic waves in the investigated glass specimens were measured using piezoelectric transducers and associated electronics (ultrasonic flaw detector USD15, Krautkramer GmbH & Co., Huerth, Germany). From the longitudinal (V_l) and transverse (V_t) sound velocities, the elastic constants were calculated using the equations described in Ref. [12]. The Vickers hardness values (HMV-2000, Shimadzu, Japan) of the

Table 2
Composition of glasses (wt.%) as determined by XRF analysis.

Glass	MgO	CaO	Na_2O	SiO_2	B_2O_3	Al_2O_3
Jd-0	19.30	28.55	–	46.04	5.89	–
Jd-20	16.50	22.82	2.96	47.24	5.86	4.78
Jd-40	11.90	17.27	5.22	50.49	5.67	9.46
Jd-60	7.72	11.76	8.63	51.40	5.75	14.71
Jd-80	3.90	5.77	11.93	53.12	5.54	19.70
Jd-100	–	–	16.85	52.30	6.58	24.23

glasses were determined at an indentation load of 1 kg and with a holding time of 15 s at full load. The reported hardness values were obtained as the average measurements from 10 indentations for each sample.

The coefficient of thermal expansion (CTE) of glasses were obtained from dilatometry measurements which were carried out on prismatic samples with dimensions 25 × mm × 5 mm × 5 mm (Netzsch DIL 402, NETZSCH-Gerätebau GmbH, Germany) at a heating rate of 5 K min^{-1}. The non-isothermal crystallization kinetics was studied using the data obtained from differential scanning calorimetry (DSC, Netzsch DSC 404, NETZSCH-Gerätebau GmbH, Germany) of glass powders carried out in air from room temperature to 1200 °C with different heating rates (β) of 5, 15, 20 and 30 K min^{-1}. The dilatometry measurements were made on a minimum of 3 samples from each composition and the standard deviation for the reported values of CTE are in the range $\pm 0.1 \times 10^{-6}$ K^{-1}.

In order to study the sintering and crystallization behavior of the investigated glass compositions, circular disc shaped pellets with Ø 20 mm and thickness ~3 mm were prepared from glass powders by uniaxial pressing (80 MPa). The pellets were sintered under non-isothermal conditions at 850 °C for 1 h. A slow heating rate (β) of 5 K min^{-1} was maintained in order to prevent deformation of the samples.

The amorphous nature of glasses and crystalline phase evolution in glass-ceramics were determined by X-ray diffraction (XRD) analysis (Rigaku Geigerflex D/Max, Tokyo, Japan; C Series; Cu K_α radiation; 2θ angle range 10–80°; step 0.02°/s). Microstructure observations were done at polished (mirror finishing) and then etched (by immersion in 2 vol.% HF solution for 2 min) surfaces of samples by field emission scanning electron microscopy (FE-SEM, Hitachi S-4100, Japan/SU-70, Hitachi, Japan) under secondary electron mode.

3. Results and discussion

3.1. Casting ability of glasses

The investigated glass compositions were readily castable after 1 h of soaking time at 1500 °C resulting in homogeneous and transparent frits. The amorphous nature of the quenched frits was confirmed by XRD analysis.

On the contrary, it was difficult to produce a stable bulk glass from composition Jd-0 as the surface of the glass rod which was in direct contact with air (and not in contact with the metallic mould) crystallized immediately after pouring the melt on the graphite mould while the remaining part of the sample did not show any tendency towards crystallization but it was prone to cracking during annealing so no experiment was done of bulk glass of Jd-0. XRD analysis reveals the formation of diopside ($CaMgSi_2O_6$; ICDD: 01-078-1390) on the surface of the glass. Similarly, in case of glass composition Jd-20, we were able to obtain a transparent and amorphous monolithic bulk glass after casting of the melt on the metallic mould. However, the glass was prone to cracking during annealing, probably due to build up of high internal stresses. Further increase in Jd/Di ratio in the glasses led to the formation of stable, transparent and monolithic bulk glasses.

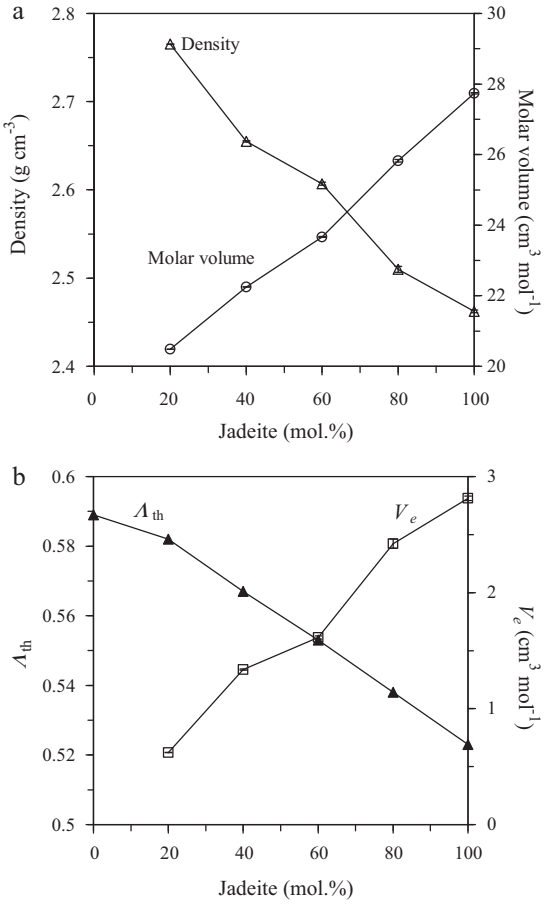

Fig. 1. (a) Density and molar volume; (b) excess volume and optical basicity of the investigated glass samples.

3.2. Density and theoretical optical basicity

3.2.1. Density and molar volume

The density of the glasses decreased with increasing Jd/Di ratio in the glasses (Fig. 1a). Since, density of a glass is an additive property and density of CaO (3.34 g cm^{-3}) and MgO (3.6 g cm^{-3}) is considerably higher than Na_2O (2.27 g cm^{-3}) and almost similar to Al_2O_3 (4.0 g cm^{-3}); therefore, decrease in density with increase in Jd content is logical.

The molar volume (V_m) and excess molar volume (V_e) were calculated using the apparent density data for the bulk glasses using following relations:

$$V_m = \frac{M}{\rho}, \tag{1}$$

where M is the molar mass of the glass and ρ is the apparent density of the bulk glasses. Similarly, excess molar volume of the glasses can be expressed as:

$$V_e = V_m - \sum_i x_i V_m(i), \tag{2}$$

Here, x_i is the molar concentration of every oxide and $V_m(i)$ is the molar volume of every oxide. The highest values of V_m and V_e were obtained for glass Jd-100 as exhibited in Fig. 1a and b, respectively. The increasing concentration of Jd in the glasses possibly increases their covalent nature due to significant addition of Al_2O_3 along with Na_2O for CaO and MgO. Al_2O_3 is known to play a dual role of glass network forming oxide as well as modifier depending on its coordination in the glass structure [13]. In the present case, Al_2O_3 is known to exist in a 4-fold coordination as has been depicted by infra-red spectroscopy results (Section 3.3). Therefore, owing to the formation of directional bonds in the structural skeleton of the glass with increasing Al_2O_3 contents, molar volume and excess volume increases [14].

3.2.2. Theoretical optical basicity (Λ_{th})

The theoretical optical basicity of the six glasses, represented by Λ_{th}, was calculated from the composition of the each glass by considering the proportion of oxygen (–II) atoms each oxide contributes (this is called as equivalent fraction, X), and also taking into account the optical basicity values of individual oxides (Λ_{RO}; RO designates various oxides in Eq. (1)) [15]. The optical basicity values as calculated using Eq. (1):

$$\Lambda_{th} = \sum X_{RO}\Lambda_{RO} \quad (3)$$

showed that Λ_{th} decreases with increase in Jd content (Fig. 1b). This decrease in Λ_{th} of glasses with increase in Jd content is due to the lower optical basicity of Al_2O_3 ($\Lambda = 0.45$) in comparison to CaO ($\Lambda = 1$) and MgO ($\Lambda = 0.69$) as the value of optical basicity of Na_2O is almost similar to that of CaO. Λ_{th} serves in the first approximation as a measure of the ability of oxygen to donate a negative charge in the glasses. It can be used to classify the covalent/ionic ratios of the glasses since an increasing Λ_{th} indicates decreasing covalency. Therefore, the results of theoretical optical basicity are in good correlation with molar volume results. According to Duffy et al. [16], who introduced the concept of theoretical optical basicity, the divalent metal ions that are stable in aqueous solution would require the glass to have an optical basicity close to that of water (i.e. $\Lambda = 0.40$). If the glass is much more basic in comparison to aqua ion, then this basicity is transmitted to the divalent ion which will then become progressively less stable. In the present investigation, Λ_{th} for all the glasses lies in the range 0.523–0.589, which is close to that of aqua ion. According to Faaland et al. [17], in silicates, an increasing amount of basic oxides will give rise to various types of structures, ranging from infinite three-dimensional frameworks, as in silica itself (SiO_2), to isolated SiO^{4-} tetrahedra in orthosilicates.

3.3. FTIR

The room temperature FTIR transmission spectra of all the four glasses are shown in Fig. 2. The spectra of all the glasses exhibit four broad transmittance bands in the region of 300–1500 cm^{-1}. This lack of sharp features is indicative of the general disorder in the silicate network mainly due to a wide distribution of Q^n (polymerization in the glass structure, where n denotes the number of bridging oxygens per SiO_4 tetrahedron) units occurring in these glasses. The most intense bands lie in the 800–1300 cm^{-1} region and are assigned to the stretching vibrations of the SiO_4 tetrahedra with a different number of bridging oxygen atoms [18,19]. A shift towards higher wave numbers has been registered in this band (~1000 cm^{-1}) with the increase in Jd content in glasses (Fig. 2), thus corresponding to a decrease in Q^2/Q^3 ratio and increasing polymerization in the glass network. Also, a small shoulder is evident ~1260–1290 cm^{-1} in all the glasses indicates towards the presence of a minor number of Q^4 units in the glasses which increase with increase in Jd content. Similar results have also been reported on diopside–jadeite-fluorapatite glasses by Abo-Mosallam et al. [2]. Further, the bands between 300 and 600 cm^{-1} region are due to bending vibrations of Si–O–Si and Si–O–Al linkages [18,19] while the transmittance bands in the 650–800 cm^{-1} region are related to the stretching vibrations of the Al–O bonds with Al^{3+} ions in four-fold coordination [18]. Furthermore, the band exhibited in IR spectra of all the glasses in the region 1300–1500 cm^{-1} corresponds to B–O vibrations in [BO_3] triangle. Since the IR band for [BO_4] tetrahedron (~1000 cm^{-1}) overlaps with that of

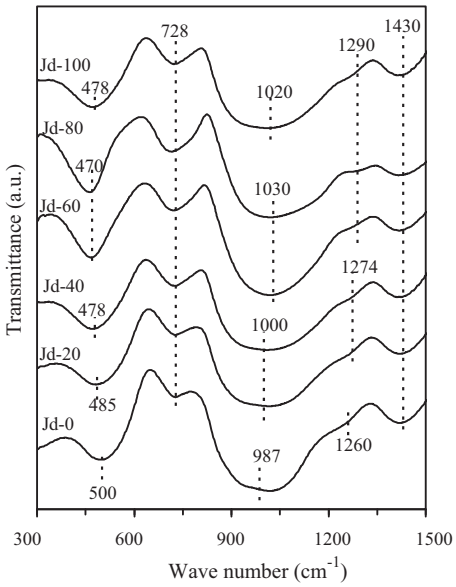

Fig. 2. FTIR spectra of the investigated glass powders.

Table 3
Mechanical properties of glasses.

Glass	E (GPa)	G (GPa)	K (GPa)	ν	H (GPa)	θ_D (K)
Jd-0	–	–	–	–	–	–
Jd-20	97.42	38.62	67.99	0.26	6.46	374
Jd-40	86.49	34.48	58.62	0.25	5.91	356
Jd-60	84.14	33.75	55.31	0.25	5.80	349
Jd-80	75.38	30.49	47.58	0.24	5.53	327
Jd-100	73.42	30.47	41.46	0.23	5.55	318

Table 4
Thermal properties of glasses.

Glasses	Jd-0	Jd-20	Jd-40	Jd-60	Jd-80	Jd-100
T_{dg} (°C)	–	651	622	607	595	570
T_s (°C)	–	701	682	671	660	633
CTE[a]	–	9.05	9.14	9.129	9.439	10.12
T_c (°C)	806	792	815	832	–	–
$T_c - T_{dg}$ (°C)	–	141	193	225	–	–
T_p (°C)	836	830	857	871	–	–
E_a (kJ mol^{-1})	500	407	356	310	–	–
n	1.072	1.416	1.654	2.07	–	–

[a] CTE × 10^6 K^{-1} (200–500 °C).

stretching vibrations of SiO_4, it could not be observed in the present investigation.

3.4. Mechanical properties of glasses

Table 3 presents the values of Vickers hardness (H) and elastic constants such as Young's modulus (E), bulk modulus (K), shear modulus (G) and Poisson's ratio (ν) and Debye temperature (θ_D) as calculated from the experimental sound velocities of the investigated Di–Jd glasses. The overall uncertainty for above calculated value is estimated to be ±2%. The values of various elastic constants decreased with increasing Jd/Di ratio in the glasses. This implies that glasses containing higher concentration of Di have rigid structure. Similarly, the values of θ_D and H are in good correlation with each other and these decreases with increase in Jd/Di ratio in the glasses which again show increases rigidity of the glass structure as shown by FTIR results (Fig. 2). Further, in order to interpret the elasticity data of glasses, both inter-atomic energies (U_0) and atomic packing densities of the various cations need to be taken into account. In the present case, ratio of (Ca + Mg)/(Na + Al) increases with decreasing Jd content in the glasses. Since, $U_{0\ Mg}$ (7.646), $U_{0\ Ca}$ (6.113) is greater than $U_{0\ Na}$ (5.139), $U_{0\ Al}$ (5.986) modulus of elasticity increases with decreases in Jd content [12]. Also, the substitution of low-valence ions by high-valence ions is better because the internal energy is proportional to the effective charge of cations and anions. Thus, the glasses containing an alkaline earth show high elastic modulus [20]. Furthermore, the decrease in the value of Poisson's ratio with increase in Jd content may be explained on the basis of 4-fold coordination of Al^{3+} in the glass structure thus decreasing the packing density of glasses [12]. As we decrease Jd/Di ratio, the amount of alkali content decreases whereas packing density increases this in turn increases Poisson's ratio, as aluminium (Al) increases Al coordination changes from 6 (small Al quantities) to 4 (Al is network forming) and network former Al decreases the atomic packing density, whereas in comparison packing density is enhanced by sixfold network modifying Al atoms. Consequently, Poisson's ratio exhibits a slight increase at low Al contents. Moreover as we increase the Jd content the connectivity of network increases as shown by FTIR analysis, So Poisson's ratio decreases because higher connectivity of network decreases the Poisson's ratio [12].

3.5. Dilatometry and differential scanning calorimetry (DSC)

The dilatometric glass transition temperature (T_{dg}) and softening point (T_s) decreased while coefficient of thermal expansion (CTE) increased with increasing of Jd/Di ratio in the glasses (Table 4). This is in contradiction with the results obtained from excess volume and infra red spectroscopy. Similar observations were reported by Abo-Mosallam et al. [2] for diopside–jadeite-fluorapatite glasses. This change in CTE is due the replacement of Ca^{2+} by Na^+ which decrease the compactness of the structure because the attraction effect of Na^+ ions on surrounding oxygen is weaker than that of Ca^{2+} ions due to high field strength of Ca^{2+} (0.35) than that of Na^+ (0.19). Thus we expected the structure become less compact with increase of Jd/Di ratio. So increase in CTE as we replace Ca^{2+} by Na^+ is due to increase in binding forces indicated by the decrease of molar volume of oxygen atoms in melts (V_0) [21]. Moreover the empirical thermal expansion factor of Na^+

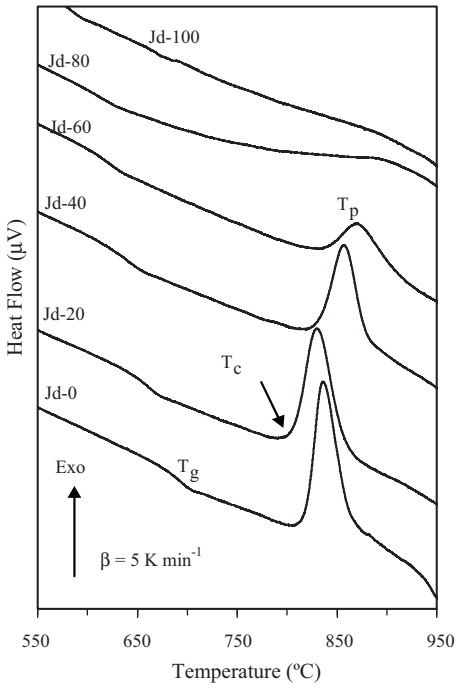

Fig. 3. Differential scanning calorimetry thermograph of the glasses at $\beta = 5$ K min^{-1}.

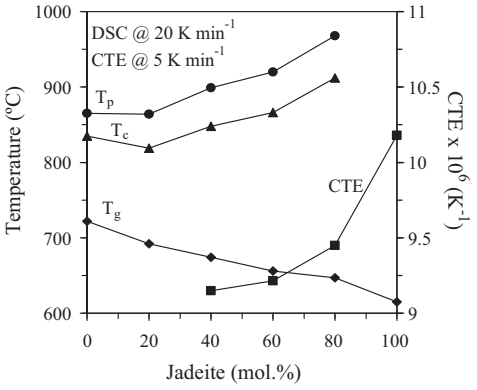

Fig. 4. Plot of T_g, T_p, T_c and CTE of the investigated glass samples.

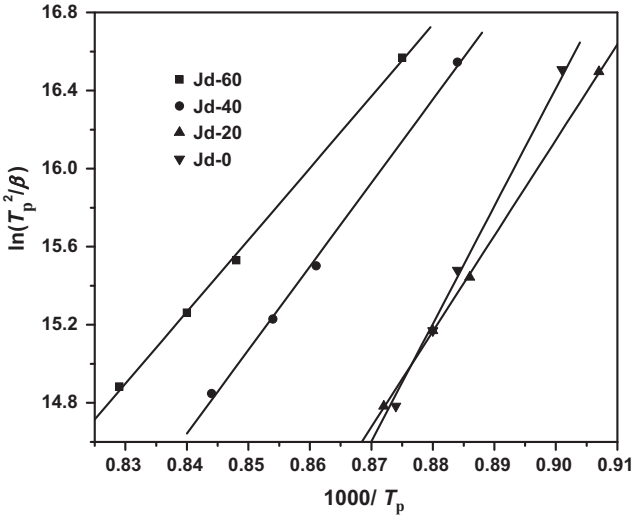

Fig. 5. Plot of E_a for all the investigated glass.

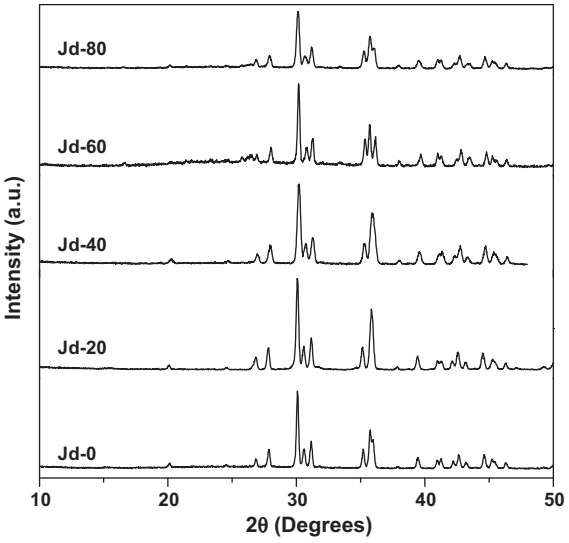

Fig. 6. X-ray diffractograms of glass-powder compacts sintered at 850 °C.

(39.5×10^{-8} °C^{-1}) is more than that of Ca^{2+} (13×10^{-8} °C^{-1}) so as we replace the Ca^{2+} by Na^{+} CTE increases whereas ionic radius of MgO is slightly larger than the AlO_4-tetrahedron and it has lower field strength in comparison to Al, but the vibrational possibilities are nearly same. The replacement of Mg^{2+} by Al^{3+} will have no or only a very small effect on the thermal expansion coefficients of investigated glasses, but Ca^{2+} has twice the field strength than that of Na^{+} it exerts much stronger forces on the surrounding oxygen ions.

The DSC scan of all the glasses (except Jd-80 and Jd-100) exhibited a single crystallization exothermic curve depicting the appearance of only one crystalline phase or simultaneous appearance of more than one phases (Fig. 3). The DSC scans for glasses Jd-80 and Jd-100 did not exhibit any crystallization exotherm as can be observed in Fig. 3 in the range of room temperature to 1200 °C. The onset temperature (T_c) and peak temperature of crystallization (T_p) decreased slightly for glass Jd-20 while they increased with further increase in Jd content at the expense of Di as is evident from Fig. 4 and Table 4. This increase in temperature at which the nucleation and crystallization start as the increase of Jd content because with the addition of Jd the amount of Al_2O_3 increase which cause an increase in the viscosity of the resultant glass melts. The result from FTIR indicated that in the present glasses Al^{3+} preferably exhibits a tetrahedral coordination. The formation of these tetrahedral AlO_4 led to increase in the viscosity of the glass which hinders the diffusion of different ions and ionic complexes, consequently, it decreases the rate of crystallization growth, and therefore, some part of sluggish crystallization of high Al_2O_3 containing glass is expected.

We investigated the non-isothermal crystallization kinetics and thermal stability of glasses using DSC. DSC thermographs

Table 5
Influence of heating rate on the thermal properties of glasses.

Glasses		Jd-0	Jd-20	Jd-40	Jd-60	Jd-80	Jd-100
β = 5 K/min	T_c	806	792	815	832	–	–
	T_p	836	830	857	871	–	–
β = 15 K/min	T_c	815	805	830	850	–	–
	T_p	857	856	890	905	–	–
β = 20 K/min	T_c	825	807	840	855	–	–
	T_p	862	875	905	922	–	–
β = 30 K/min	T_c	828	807	850	862	–	–
	T_p	880	890	915	928	–	–

for all the six glasses were taken at different heating rates (β = 5, 15, 20 and 30 K/min). The values of T_c and T_p shifted towards higher side with increasing in heating rate (Table 5). To calculate the activation energy of crystallization, the experimental results of DSC with different heating rates (β = 5 K/min, 15 K/min, 20 K/min, and 30 K/min) were applied in the modified forms of Kissinger (Eq. (4)) equation:

$$\ln\left(\frac{T_p^2}{\beta^n}\right) = \frac{E_a}{RT_p} + \text{constant} \quad (4)$$

where n is the Avrami constant. The value of n is given in Table 4. Experimental results of Eq. (4), for the investigated glasses are shown in Fig. 5. The values of E_a, calculated from these plots by using the linear least square fitting of the experimental data, are presented in Table 4.

The activation energy of crystallization (E_a) decreased monotonically with increase of Jd/Di ratio in the glasses (Table 4). The value of Avrami parameter for all the glasses exhibited intermediate mechanism of crystallization as depicted in Table 4. Well sintered and dense glass powder compacts were obtained for all the glass compositions after sintering at 850 °C for 1 h. However, the viscosity of glass powder compacts decreased considerably with increasing Jd content in the glasses, thus, leading to the rounding of edges of the circular discs. Diopside (01-078-1390) crystallized as the only crystal-

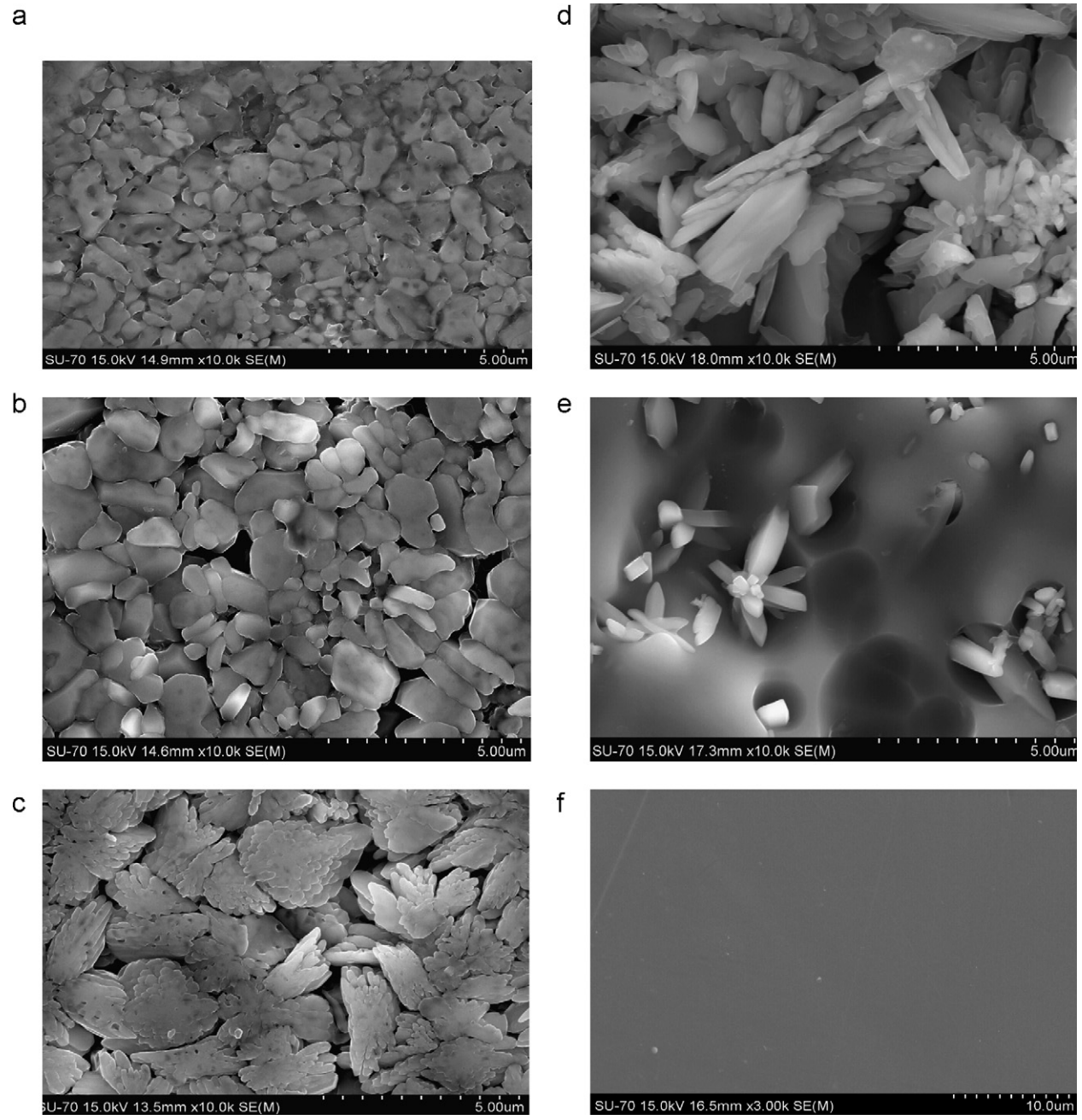

Fig. 7. SEM images on polished surfaces of glass-ceramics crystallized at 850 °C: (a) Jd-0; (b) Jd-20; (c) Jd-40; (d) Jd-60; (e) Jd-80; (f) Jd-100.

line phase in investigated glass-ceramics (Fig. 6) except Jd-100 which is amorphous as shown in SEM image in Fig. 7(f), thus depicting the formation of a solid solution as has also been reported by Abo-Mosallam et al. [2]. However, some unidentified diffraction peaks were observed in investigated glass-ceramics except Jd-100. The SEM images as shown in Fig. 7 shows that the amount of crystal phase formed increase with decreasing the Jd content so we have maximum crystalline phase in Jd-0 whereas Jd-100 is totally amorphous which implies that the crystalline phase in glass is diopside and residual glass has a jadeite composition. Therefore, it will be interesting to make a quantitative analysis of the crystalline phases present in these glass-ceramics through Rietveld refinement analysis of XRD data.

4. Conclusions

In conclusion, the structure, crystallization behavior and mechanical characterization of glasses along Di–Jd join has been investigated. The V_m, V_e and CTE increase while density, elastic constants, hardness, Λ_{th} and T_{dg} decreases with an increase of Jd/Di ratio. The polymerization in the glass structure increases with increase of Jd/Di ratio. E_a decreased with increase of Jd/Di ratio.

References

[1] N. Morimoto, Nomenclature of pyroxenes, Am. Miner. 73 (1988) 1123–1133.
[2] H.A. Abo-Mosallam, R.G. Hill, N. Karpukhina, R.V. Law, MAS-NMR studies of glasses and glass-ceramics based on clinopyroxene–fluorapatite system, J. Mater. Chem. 20 (2010) 790–797.
[3] J.F. Schairer, H.S. Yoder Jr., The nature of residual liquids from crystallization, with data on the system nepheline–diopside–silica, Am. J. Sci. 258-A (1960) 273–283.
[4] P.M. Bell, J. Kalb, Stability of ompbacite in the absence of excess silica, Carnegie Inst. Wash. Year 67 (1969) 97–98.
[5] T.J.B. Holland, The experimental determination of activities in disordered and short-range ordered jadeitic pyroxenes, Contrib. Mineral. Petrol. 82 (1983) 214–220.
[6] T. Gasparik, Diopside–jadeite join at 16–22 GPa, Phys. Chem. Miner. 23 (1996) 476–486.
[7] T. Gasparik, Experimentally determined compositions of diopside–jadeite pyroxene in equilibrium with albite and quartz at 1200–1350 °C and 15–34 kbar, Geochim. Cosmochim. Acta 49 (1985) 865–870.
[8] L. Liu, Phase relations in the system diopside–jadeite at high pressures and high temperatures, Earth Planet Sci. Lett. 47 (1980) 398–402.
[9] B.J. Wood, T.J.B. Holland, R.C. Newton, O.J. Kleppa, Thermochemistry of jadeite–diopside pyroxenes, Geochim. Cosmochim. Acta 44 (9) (1980) 1363–1371.
[10] D. Wang, Effect of crystallization on the property of hard enamel coating on steel substrate, Appl. Surf. Sci. 255 (8) (2009) 4640–4645.
[11] A. Goel, D.U. Tulyaganov, V.V. Kharton, A.A. Yaremchenko, S. Eriksson, J.M.F. Ferreira, Optimization of La_2O_3-containing diopside based glass-ceramic sealants for fuel cell applications, J. Power Sources 189 (2009) 1032–1043.
[12] T. Rouxel, Elastic properties and short-to medium-range order in glasses, J. Am. Ceram. Soc. 90 (10) (2007) 3019–3039.
[13] N. Lahl, K. Singh, L. Singheiser, K. Hilpert, D. Bahadur, Crystallization kinetics in AO–Al_2O_3–SiO_2–B_2O_3 glass (A=Ba, Ca, Mg), J. Mater. Sci. 35 (2000) 3089.
[14] J.W. Martin, Concise Encyclopedia of the Structure of Materials, Elsevier Science Ltd., UK, 2006, , ISBN: 978-0-08-045127-5.
[15] V. Dimitrov, S. Sakka, Classification of simple oxides: a polarizability approach, J. Appl. Phys. 79 (1996) 1736.
[16] J.A. Duffy, M.D. Ingram, S. Fong, The electronic polarisability of oxygen in glass and the effect of composition, Phys. Chem. Chem. Phys. 2 (2000) 1829.
[17] S. Faaland, M.-A. Einarsrud, T. Grande, Reactions between calcium and strontium substituted lanthanum cobaltite ceramic membranes and calcium silicate as sealing materials, Chem. Mater. 13 (2001) 723–732.
[18] S.-L. Lin, C.-S. Hwang, Structures of CeO_2–Al_2O_3–SiO_2 glasses, J. Non-Cryst. Solids 202 (1996) 61–67.
[19] J.T. Kohli, R.A. Condratr, J.E. Shelby, Raman and infrared spectra of rare earth aluminosilicate glasses, Phys. Chem. Glasses 34 (1993) 81–87.
[20] N. Soga, Elastic moduli and fracture toughness of glass, J. Non-Cryst. Solids 73 (1985) 305–313.
[21] H. Taniguchi, T. Marase, Some physical properties and melt structures in the system diopside–anorthite, J. Volcan. Geo. Res. 34 (1987) 51–64.